NeuroImage 54 (2011) 517–527

Contents lists available at ScienceDirect

NeuroImage

journal homepage: www.elsevier.com/locate/ynimg

Low frequency fluctuations reveal integrated and segregated processing among the cerebral hemispheres

Dylan G. Gee [a], Bharat B. Biswal [b,c], Clare Kelly [a], David E. Stark [d], Daniel S. Margulies [e], Zarrar Shehzad [a], Lucina Q. Uddin [f], Donald F. Klein [a,b], Marie T. Banich [g], F. Xavier Castellanos [a,b], Michael P. Milham [a,b,*]

[a] Phyllis Green and Randolph Cōwen Institute for Pediatric Neuroscience at the NYU Langone Medical Center, New York, NY 10016, USA
[b] Nathan Kline Institute for Psychiatric Research, Orangeburg, NY 10962, USA
[c] Department of Radiology, University of Medicine and Dentistry of New Jersey, Newark, NJ 07101, USA
[d] Harvard Medical School, Boston, MA 02115, USA
[e] Berlin School of Mind and Brain, Humboldt Universität 10099 Berlin, Germany
[f] Department of Psychiatry, Stanford University School of Medicine, Stanford, CA 94304, USA
[g] Department of Psychology, University of Colorado, Boulder, CO 80309, USA

ARTICLE INFO

Article history:
Received 5 February 2010
Revised 24 May 2010
Accepted 26 May 2010
Available online 4 June 2010

ABSTRACT

Resting-state functional magnetic resonance imaging (fMRI) has provided a novel approach for examining interhemispheric interaction, demonstrating a high degree of functional connectivity between homotopic regions in opposite hemispheres. However, heterotopic resting-state functional connectivity (RSFC) remains relatively uncharacterized. In the present study, we examine non-homotopic regions, characterizing heterotopic RSFC and comparing it to intrahemispheric RSFC, to examine the impact of hemispheric separation on the integration and segregation of processing in the brain. Resting-state fMRI scans were acquired from 59 healthy participants to examine inter-regional correlations in spontaneous low frequency fluctuations in BOLD signal. Using a probabilistic atlas, we correlated probability-weighted time series from 112 regions (56 per hemisphere) distributed throughout the entire cerebrum. We compared RSFC for pairings of non-homologous regions located in different hemispheres (heterotopic connectivity) to RSFC for the same pairings when located within hemisphere (intrahemispheric connectivity). For positive connections, connectivity strength was greater within each hemisphere, consistent with integrated intrahemispheric processing. However, for negative connections, RSFC strength was greater between the hemispheres, consistent with segregated interhemispheric processing. These patterns were particularly notable for connections involving frontal and heteromodal regions. The distribution of positive and negative connectivity was nearly identical within and between the hemispheres, though we demonstrated detailed regional variation in distribution. We discuss implications for leading models of interhemispheric interaction. The future application of our analyses may provide important insight into impaired interhemispheric processing in clinical and aging populations.

Introduction

Resting-state functional connectivity (RSFC) analyses of fMRI data provide a powerful and efficient method of mapping neuronal circuits that have proven difficult to examine using traditional task-based fMRI approaches. In particular, RSFC analyses provide fresh insights into interhemispheric connectivity.

The ability of RSFC analyses to detect robust patterns of interhemispheric connectivity was first demonstrated within the motor system (Biswal et al., 1995). Since then, studies have revealed robust patterns of correlated spontaneous activity between homologous regions in opposite hemispheres (homotopic connectivity) (Fair et al., 2008; Hagmann et al., 2008; Margulies et al., 2007; Salvador et al., 2005; Stark et al., 2008).

Whereas these studies examined homotopic functional relationships, interhemispheric connections between non-homologous regions in opposite hemispheres (heterotopic connectivity) remain less well understood. Although recent fMRI studies have noted that heterotopic brain regions exhibit robust functional relationships (Hagmann et al., 2008; Salvador et al., 2005; Stark et al., 2008), no study has directly examined or characterized patterns of heterotopic connectivity. The present study focuses on heterotopic connectivity directly, as well as in comparison to intrahemispheric connectivity.

* Corresponding author. 215 Lexington Ave, 14th Floor, New York, NY 10016, USA. Fax: +1 212 263 4675.
E-mail address: michael.milham@nyumc.org (M.P. Milham).

1053-8119/$ – see front matter © 2010 Elsevier Inc. All rights reserved.
doi:10.1016/j.neuroimage.2010.05.073

We compared the strength of functional connectivity between distinct anatomical regions in opposite hemispheres (heterotopic connectivity) to the strength of functional connectivity between the same regions in the same hemisphere (intrahemispheric connectivity).

Analyses of interhemispheric connectivity can inform models of how interhemispheric interactions affect cognitive processing. Some models suggest that interhemispheric interaction aids information processing by coordinating parallel processing between the hemispheres (Banich and Brown, 2000). Other models posit that lateralization of function allows competing processes to be insulated from each other (Kosslyn et al., 1992; Liederman, 1986). While the ubiquitous finding of homotopic symmetry is consistent with models of coordinated interhemispheric processing (Banich, 2003), interhemispheric segregation models have not been tested using RSFC.

We approach heterotopic connectivity through a comparison of inter- and intrahemispheric RSFC (Stark et al., 2008; Liu et al., 2009) associated with 112 regions-of-interest (ROIs; 56 per hemisphere) encompassing the entire cerebrum. For each possible pairing of these ROIs (referred to as a regional pairing), we examined differences in heterotopic and intrahemispheric connectivity for distinct anatomical regions both with respect to the strength and distribution of significant positive and negative connections. Within the intrahemispheric pairings, we tested for potential hemispheric asymmetries (i.e., differences in the strength and distribution of RSFC within the left versus right hemisphere). We also tested for hemispheric differences in the strength and distribution of RSFC according to lobe and functional hierarchy (Mesulam, 2000) (i.e., primary, unimodal, heteromodal, paralimbic, limbic, and subcortical).

Several authors hypothesize that positive RSFC reflects coordinated or integrated processing within functional systems, whereas negative connectivity appears to be associated with segregated, separable, or competing systems (Fair et al., 2007; Fox et al., 2005; Kelly et al., 2008). We considered interhemispheric connectivity from the perspective that processing in the two hemispheres is at least partially segregated. Therefore, we predicted that negative connectivity would be greater between hemispheres, while positive connectivity would be greater within hemispheres. Additionally, we used lobar- and functional hierarchy-based regional classifications to investigate regional differences in intrahemispheric and heterotopic connectivity. As models of interhemispheric interaction do not make explicit predictions about regional variation, this aspect of the study was exploratory.

Materials and methods

The present work represents a novel analysis of the dataset employed in our recent study on homotopic interhemispheric RSFC (Stark et al., 2008). Participant characteristics, data acquisition, preprocessing, and time series extraction methods have been updated to reflect our most current analytic path. Details are provided below.

Participants

Participants included 59 right-handed volunteers (28 males, 31 females, ages 19–49, mean age 29.2 ± 7.9 years) with no history of psychiatric or neurological illness as confirmed by psychiatric clinical assessment. Informed consent was obtained prior to participation, and participants received monetary compensation for their involvement. Data collection was carried out according to protocols approved by the institutional review boards of New York University (NYU) and the NYU School of Medicine, with Dr. F. Xavier Castellanos as principal investigator and Drs. Milham, Gee and colleagues as co-investigators.

Data acquisition

Functional imaging data were acquired using a Siemens Allegra 3.0 Tesla scanner equipped for echo planar imaging (EPI). For each participant, we obtained a resting-state scan consisting of 197 contiguous EPI whole-brain functional volumes, resulting in a 6 min 38 s scan (TR = 2000 ms; TE = 25 ms; flip angle = 90°, 39 slices, matrix = 64 × 64; FOV = 192 mm; acquisition voxel size = 3 × 3 × 3 mm). Participants were instructed to relax and remain still with their eyes open. A high resolution T1-weighted anatomical image was also acquired using a magnetization prepared gradient echo sequence (MPRAGE; TR = 2500 ms; TE = 4.35 ms; TI = 900 ms; flip angle = 8°, 176 slices; FOV = 256 mm) for spatial normalization and localization.

Image preprocessing

Slice timing correction (for interleaved acquisition), motion correction, despiking, temporal band pass filtering (0.005–0.1 Hz), and quadratic detrending using linear least squares were performed using Analysis of Functional NeuroImaging (AFNI) (http://afni.nimh.nih.gov/afni). Mean-based intensity normalization of all volumes by the same factor (each subject's entire four-dimensional (4-D) dataset was scaled by its global mean) was performed using fMRIb Software Library (FSL) (www.fmrib.ox.ac.uk).

The data were not spatially smoothed, as this is effectively achieved via averaging across all voxels within each ROI (see below), and because we wanted to minimize artifactual interhemispheric correlation due to smoothing across the medial wall. Registration of high resolution structural images to the MNI152 template (Montreal Neurological Institute) with 2 mm^3 resolution was carried out using the FSL linear registration tool FLIRT (Jenkinson and Smith, 2001; Jenkinson et al., 2002). Transformation to MNI152 standard space was then further refined using FNIRT nonlinear registration (Andersson et al., 2007a,b). Linear registration of each participant's functional time series to the space of the high resolution structural image was also carried out using FLIRT.

Nuisance signal regression

To control for the effects of physiological processes (such as fluctuations related to cardiac and respiratory cycles), and motion, we removed signal associated with several nuisance covariates. Specifically, we regressed each subject's 4-D volume on nine predictors that modeled nuisance signals from white matter (WM), CSF, the global signal, and six motion parameters, as detailed elsewhere (see e.g., Kelly et al., 2009). In a supplementary analysis that examined the dependence of our findings on global signal regression, we repeated the nuisance signal regression step using the same nuisance predictors, with the exception of the global signal.

This nuisance signal regression step produced a 4-D residuals volume for each participant. As a final preprocessing step, each participant's time series was spatially normalized by applying the previously computed transformation to MNI152 standard space, with 2 mm^3 resolution.

Time series extraction

Parcellation of functional data was carried out using the Harvard–Oxford Structural Atlas, a validated probabilistic atlas implemented in FSL that divides each hemisphere into regions corresponding to portions of cortical gyri and subcortical gray matter nuclei (Kennedy et al., 1998; Makris et al., 1999). ROIs were generated for 112 regions (56 in each hemisphere), covering the entire cerebrum (Fig. 1A). In order to minimize effects due to inter-individual anatomic variability, atlas-derived values corresponding to each voxel's probability of inclusion in a given region were used to weight each voxel's time series within that region. For each participant, mean time series were

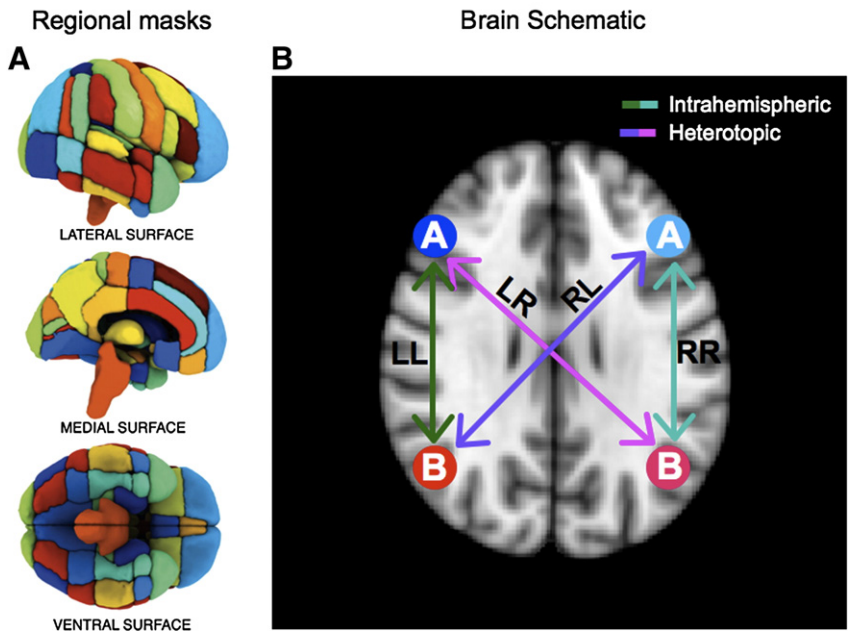

Fig. 1. (A) Regional masks. A total of 112 regional masks (56 in each hemisphere) comprising the entire cerebrum were generated from the Harvard–Oxford Structural Atlas, a validated probabilistic atlas that divides each hemisphere into regions corresponding to portions of cortical gyri and subcortical gray matter nuclei. Atlas-derived values corresponding to each voxel's probability of inclusion in a given region were used to derive probability-weighted time series for all 112 regions. For visualization, all three-dimensional reconstructions are thresholded to include voxels with >25% probability of inclusion in a given region. (Reproduced from Stark et al., 2008 with permission from the Society for Neuroscience © 2008). (B) Brain schematic. Intrahemispheric connections are defined as those between distinct anatomical regions (A, B) located within the same hemisphere (LL = regions A and B are in the left hemisphere; RR = regions A and B are in the right hemisphere). Heterotopic connections are defined as those between distinct anatomical regions located in opposite hemispheres (LR = region A is in the left hemisphere and B in right; RL = region A is in the right hemisphere and B in left). To determine the impact of interhemispheric separation, we contrasted intrahemispheric and heterotopic connectivity (LL vs. LR, LL vs. RL, RR vs. LR, and RR vs. RL).

extracted from the standard space 4-D residuals volume for each ROI by averaging across the probability-weighted time series for all voxels with >25% probability of inclusion within that ROI. This step generated 112 time series representing every cortical and subcortical region for each of the 59 participants.

Correlational analyses

All further analyses were conducted in MATLAB 7.4. For each participant, we calculated the correlation between every pairing of time series from the set of 112 brain regions. There were 6216 possible connections, 56 of which represented homotopic connections, 3080 heterotopic connections, 1540 within-left hemisphere connections, and 1540 within-right hemisphere connections. Using Pearson correlation (z-transformed), RSFC was calculated for all possible non-homotopic pairs. The average time series for each region (averaged across all voxels in the region) was correlated with the average time series for every other region in the same hemisphere (intrahemispheric) and for every heterotopic region in the contralateral hemisphere (interhemispheric). Therefore, for any given pair of regions (X, Y), four possible hemispheric configurations existed: two intrahemispheric (LL: X in left, Y in left; RR: X in right, Y in right) and two heterotopic (LR: X in left, Y in right; RL: X in right, Y in left) (Fig. 1B).

Significant connections were identified using a one-sample t-test for each pair (Bonferroni corrected; $p<[0.05/6160]$), and only connections passing this significance threshold were analyzed further.

Strength

Heterotopic (LR and RL) versus intrahemispheric (LL and RR)

Given our hypotheses of greater negative connectivity between the hemispheres, and greater positive connectivity within, we tested for the presence of possible differences in overall positive and negative connectivity strength between heterotopic and intrahemispheric configurations. Specifically, we 1) calculated the mean connectivity strength (positive and negative separately) across eligible regional pairings for each participant for each configuration, and 2) carried out paired t-tests to compare connectivity strength (positive and negative separately) within each hemisphere (LL, RR) with its corresponding heterotopic configuration (LR, RL) as follows: LL vs. LR, LL vs. RL, RR vs. RL, RR vs. LR. In order to examine potential hemispheric asymmetries, we also tested for potential differences with respect to within-hemisphere connectivity (LL vs. RR). Negative connectivity strengths were multiplied by −1, so that larger values for both positive and negative connectivity indicated greater strength.

Individual connections

Given that the relative strengths of intrahemispheric and heterotopic connections may differ among regional pairings, we further analyzed RSFC strength for intrahemispheric versus heterotopic RSFC strength at the level of each individual regional pairing. Specifically, for each regional pairing that was significantly connected in at least one of the hemispheric configurations, we carried out paired t-tests comparing each intrahemispheric configuration with each heterotopic configuration (Bonferroni corrected). In order to summarize significant differences in RSFC strength for intrahemispheric and heterotopic connections, we created two *relative dominance indices* (RDI) for each regional pairing, one intrahemispheric and the other heterotopic. Specifically, for each regional pairing, the *intrahemispheric RDI* is defined as the number of intrahemispheric configurations that were significantly greater than their heterotopic counterparts (*intrahemispheric RDI* = [LL>LR] + [LL>RL] + [RR>LR] + [RR>RL]; score range: 0–4); the *heterotopic RDI* is defined as the number of heterotopic configurations that were significantly greater than their intrahemispheric counterparts (*heterotopic RDI* = [LR>LL] + [LR>RR] + [RL>LL] + [RL>RR]; score range: 0–4). We used a chi-square test in order to compare intrahemispheric versus heterotopic configurations with respect to the distribution of RDI values. See supplemental materials for an alternative summary index that characterizes the relative strength of each of the

four hemispheric configurations (LL, LR, RL, and RR) for each regional pairing and yields similar results (Supplemental methods; Supplemental results; Supplemental Figs. 1–4; Supplemental Tables 2–3).

Distribution

Although our hypotheses primarily focus on differences in the connectivity strength between heterotopic and intrahemispheric connections, differences in the distribution of positive and negative connections may exist between heterotopic and intrahemispheric configurations as well. To explore this possibility, we examined the extent to which the four hemispheric configurations (LL, RR, LR, and RL) differ with respect to the distribution of positive and negative connections. To do so, we determined whether the correlation for each regional pairing was significantly different from zero (Bonferroni corrected; $p<[0.05/6160]$), for each of the four possible hemispheric configurations (LL, LR, RL, and RR). If a connection was not significant in any of the four hemispheric configurations, it was not included in analyses of distribution. However, if a unique regional pairing exhibited a significant correlation for any one of the four hemispheric configurations, we examined whether it was positive, negative, or non-significant in each of the hemispheric configurations. We used this information to calculate percentages of positive, negative, and non-significant connections by hemispheric configuration. Given the stringent Bonferroni correction employed, a connection could erroneously be declared absent due to type II error. In order to guard against such type II errors, we considered a connection absent for a hemispheric configuration only if it (1) failed to reach significance with the uncorrected alpha = 0.05 threshold, and (2) differed significantly ($p<0.05/3$; correction based on maximal number of alternative configurations that could be significantly connected for a given regional pairing) from those hemispheric configurations deemed to be present for a regional pairing.

Connection classification strategies

Given the vast number of significant connections in the brain, even after Bonferroni correction, we characterized regional connectivity (i.e., region A and region B) using two regional classification strategies in order to capture properties that may explain regional variation in RSFC strength: (1) lobar grouping, and (2) functional hierarchy. When classifying by lobe, we sorted regions into frontal, temporal, parietal, occipital, and subcortical groups. When classifying by functional hierarchy, we sorted regions into primary, unimodal, heteromodal, paralimbic, limbic, and subcortical groups. The hierarchical groupings are derived from anatomical, electrophysiological, behavioral, lesion, and functional imaging studies in non-human primates and in humans (Mesulam, 2000). (See Table 1 for the number of regions in each classification, and Supplemental Table 1 for a complete listing of each region's lobar and functional classification).

Table 1
Regional classifications.

Lobar classification		Functional hierarchy classification	
Regional group	# of regions	Regional group	# of regions
Frontal	15	Primary	5
Temporal	11	Unimodal	22
Parietal	14	Heteromodal	12
Occipital	10	Paralimbic	9
Subcortical	6	Limbic	2
		Subcortical	6

In order to examine regional variation in the strength and distribution of RSFC, we grouped regions by lobe and by functional hierarchy level.

Inter-regional distance

In order to investigate inter-regional distance as a potential confound, we conducted analyses to determine the relationship between inter-regional distance and functional connectivity. First, we tested the relationship between distance and intrahemispheric RSFC using correlation. Then we tested the relationship between distance and heterotopic connectivity. To do so, we 1) calculated the additional distance for the interhemispheric connection versus the intrahemispheric connection between two regions (i.e., interhemispheric [A, B]–intrahemispheric [A, B]), then 2) examined the relationship between this additional distance and the difference in RSFC between the two configurations (i.e., interhemispheric r–intrahemispheric r). We then verified our findings by carrying out a multiple regression analysis with distance and hemispheric configuration as independent predictors.

Results

Identification of significant connections

For all possible non-homotopic connections in the brain, RSFC strength was calculated using Pearson correlation (z-transformed), and significant connections were identified using a one-sample t-test for each pair ($p<0.05$, Bonferroni corrected). Using this method, 2324 significant connections were identified out of 6160 possible connections. For each pairing of the 56 anatomical regions, four distinct hemispheric configurations exist: left–left (LL), left–right (LR), right–left (RL), and right–right (RR). Next, defining *eligible regional pairings* as those pairings for which at least one of the four possible hemispheric configurations (LL, LR, RL, and RR) was significantly connected (1540 possible pairings), 410 eligible positive regional pairings and 377 eligible negative pairings were identified.

Strength of positive and negative connections

Intrahemispheric vs. heterotopic RSFC strength: overall

For both positive and negative regional pairings (410 positive and 377 negative), paired t-tests were carried out comparing mean connectivity strength across the eligible pairings between corresponding intrahemispheric (LL and RR) and heterotopic (LR and RL) configurations (positive and negative analyzed separately). Analyses revealed highly significant differences between intrahemispheric and heterotopic configurations (Fig. 2), with (1) intrahemispheric configurations exhibiting greater positive connectivity than heterotopic configurations (LL>RL: $p<1.0\times10^{-26}$; LL>LR: $p<1.0\times10^{-25}$; RR>LR: $p<1.0\times10^{-27}$; RR>RL: $p<1.0\times10^{-25}$), and (2) heterotopic configurations exhibiting greater negative connectivity than their corresponding intrahemispheric configurations (RL>LL: $p<1.0\times10^{-19}$; LR>LL: $p<1.0\times10^{-10}$; RL>RR: $p<1.0\times10^{-10}$; LR>RR: $p<1.0\times10^{-11}$). The two intrahemispheric configurations (LL, RR) did not differ significantly in positive or negative mean connectivity strength.

We considered the possibility that stringency of the Bonferroni correction could limit the generalizability of our results to less robust connections. Accordingly, we repeated our analyses using the false discovery rate ($q=0.05$) approach, which increased the number of significant regional pairings by about 50%. There were no notable changes in the patterns of connectivity (Supplemental Fig. 5). Thus, data reported here correspond to the more conservative Bonferroni corrections.

Intrahemispheric vs. heterotopic RSFC strength: region level

Positive connectivity. Analysis of intrahemispheric and heterotopic RDI indices for positive regional pairings revealed that the majority of intrahemispheric configurations exhibited dominance over 1 or more

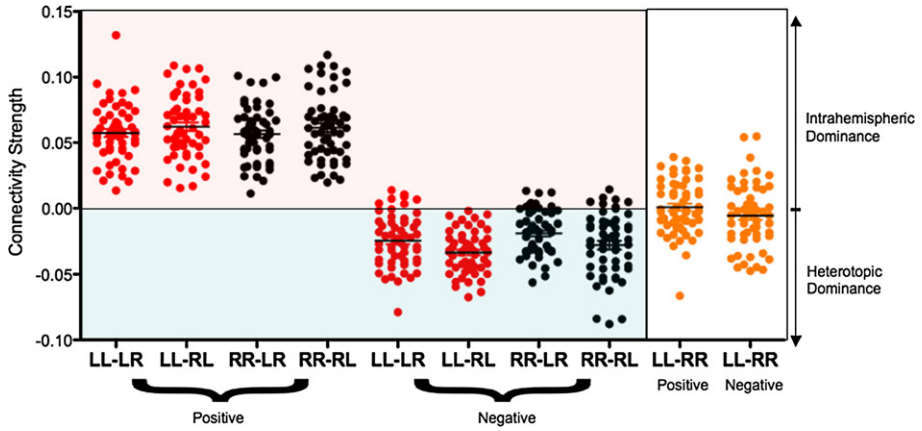

Fig. 2. Differences in mean connectivity strengths. In order to test for differences in the connectivity strength of intrahemispheric versus heterotopic RSFC, for each participant, we first calculated the mean connectivity strength across eligible regional pairings (positive and negative separately) for each of the four hemispheric configurations (LL, LR, RL, and RR). For both positive and negative connectivity, we then carried out pairwise t-tests (paired variable = participant; degrees of freedom = 58) to examine differences in the mean RSFC strength between the hemispheric configurations. Intrahemispheric configurations demonstrated greater positive connectivity than heterotopic configurations (LL>RL: $p<1.0\times10^{-26}$; LL>LR: $p<1.0\times10^{-25}$; RR>LR: $p<1.0\times10^{-27}$; RR>RL: $p<1.0\times10^{-25}$), whereas heterotopic configurations demonstrated greater negative connectivity than their corresponding intrahemispheric configurations (RL>LL: $p<1.0\times10^{-19}$; LR>LL: $p<1.0\times10^{-10}$; RL>RR: $p<1.0\times10^{-10}$; LR>RR: $p<1.0\times10^{-11}$). This figure also demonstrates within-hemisphere comparisons (i.e., LL>RR and RR>LL). Note: (1) eligible regional pairings are defined as those for which at least one of the four possible hemispheric configurations was significantly connected ($p<0.05$, Bonferroni corrected; positive or negative), and (2) in order to facilitate visual comparison with positive connectivity strength, negative connectivity strengths were multiplied by −1, so that larger values for both positive and negative indicate greater connectivity strength.

of their corresponding heterotopic configurations (Fig. 3). Specifically, 56.8% of positive regional pairings had intrahemispheric RDIs of 1 or higher (1: 23.4%, 2: 12.7%, 3: 10.0%, and 4: 10.7%). By contrast, 4.9% of positive regional pairings had a heterotopic RDI = 1 and none had heterotopic RDI > 1. See Table 2 for a tabulation of RDIs. When sorted by lobe, positive pairings within the hemispheres between frontal and temporal regions, frontal and parietal regions, and temporal and parietal regions, demonstrated an intrahemispheric RDI of 1 or higher (Fig. 4), indicating an asymmetry in the strength of one or more configurations. Frontal regions were also strongly connected with other frontal regions within the hemispheres, with a similar pattern for temporal, parietal, and occipital regions. When grouped by hierarchical classification, the strongest positive correlations were demonstrated between the following hierarchical groupings: unimodal with other unimodal, unimodal with heteromodal, unimodal with paralimbic, heteromodal with other heteromodal, and heteromodal with paralimbic regions (Fig. 5).

Negative connectivity. Analysis of intrahemispheric and heterotopic RDI indices of relative connectivity strength for negative regional pairings found that a substantial proportion of regional pairings exhibited heterotopic dominance (Fig. 3). Specifically, 31.3% of negative connections had heterotopic RDIs of 1 or higher (1: 16.7%, 2: 9.5%, 3: 3.5%, and 4: 1.6%), whereas only 3.7% of negative regional pairings had an intrahemispheric RDI = 1. The strongest negative correlations were exhibited between the following lobar groupings: frontal with other frontal, frontal with temporal, frontal with parietal, frontal with occipital, and temporal with parietal regions (Fig. 4). When sorted by functional hierarchy, the strongest negative correlations were found between the following groupings: unimodal with heteromodal, unimodal with paralimbic, heteromodal with other heteromodal, and heteromodal with paralimbic regions (Fig. 5). In addition, the distribution of RDI values for intrahemispheric and heterotopic connections differed significantly (intrahemispheric: χ^2 (4) = 261, $p<0.000001$; heterotopic: χ^2 (4) = 102, $p<0.000001$).

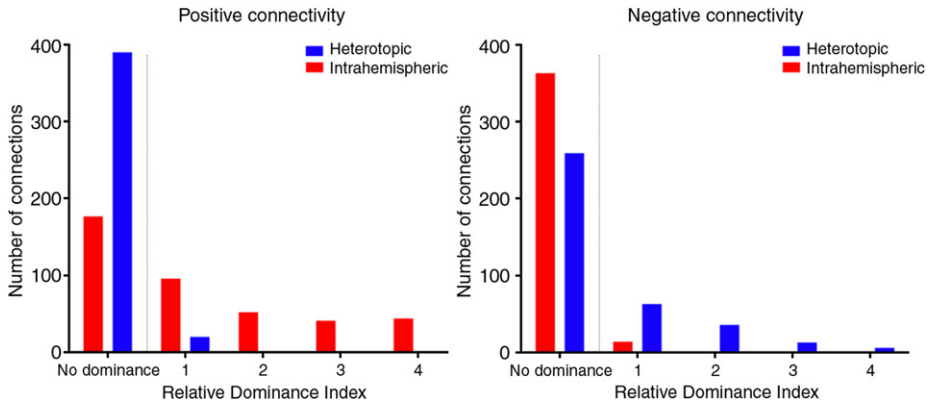

Fig. 3. Intrahemispheric versus heterotopic RSFC strength. The *relative dominance index* (RDI) was developed to compare intrahemispheric versus heterotopic RSFC strength at the level of each individual connection. For each eligible regional pairing that was significantly connected in at least one of the hemispheric configurations, we carried out paired t-tests comparing each intrahemispheric configuration with each heterotopic configuration (Bonferroni corrected). Then, for each regional pairing, t-test results were used to calculate: (1) the *intrahemispheric RDI*, defined as the number of intrahemispheric configurations that were greater than their heterotopic counterparts ([LL>LR] + [LL>RL] + [RR>LR] + [RR>RL]), and (2) the *heterotopic RDI*, defined as the number of heterotopic configurations that were greater than their intrahemispheric counterparts ([LR>LL] + [RL>LL] + [LR>RR] + [RL>RR]). RDI analyses demonstrated greater dominance for positive connectivity among intrahemispheric connections, and greater dominance for negative connectivity among heterotopic connections.

Table 2
Intrahemispheric and heterotopic relative dominance indices.

RDI	Intrahemispheric N (%)	Heterotopic N (%)
Positive connectivity		
4	44 (10.7)	0 (0)
3	41 (10.0)	0 (0)
2	52 (12.7)	0 (0)
1	96 (23.4)	20 (4.9)
0	177 (43.2)	390 (95.1)
Negative connectivity		
4	0 (0)	6 (1.6)
3	0 (0)	13 (3.5)
2	0 (0)	36 (9.5)
1	14 (3.7)	63 (16.7)
0	363 (96.3)	259 (68.7)

The *relative dominance index* (RDI) provides a measure of intrahemispheric versus heterotopic RSFC strength at the level of each individual connection. Here we tabulate the number of positive and negative connections exhibiting each level of intrahemispheric and heterotopic RDI.

Distribution of positive and negative connections

Hemispheric configurations

Our distribution analyses revealed highly similar patterns of positive and negative connectivity across all four hemispheric configurations. Significant connectivity within a hemisphere typically was accompanied by significant connectivity between the hemispheres (true for 90% of positive pairings, 85% of negative pairings). For example, for two regions A and B, if A in the left hemisphere was significantly positively connected to B in the left hemisphere, then A in the left hemisphere was significantly positively connected to B in the right hemisphere. For the remaining pairings (10% of positive pairings and 15% of negative pairings), connectivity was significant in one of the configurations but not in the other. However, these remaining pairings did not differ in the direction (i.e., positive or negative) of their connectivity. (See Supplemental Fig. 6 for overall distribution of positive, negative, and non-significant pairings).

Lobar classification

Lobar groupings demonstrated differential patterns in the proportion of positive and negative connections between regions (Fig. 6). Within a given lobe, the majority of significantly connected pairings exhibited positive connectivity. The preponderance of negative connections was demonstrated between frontal and parietal and between frontal and occipital pairings. We noted a low degree of connectivity between subcortical and cortical regions. Among the connections detected with subcortical regions, positive connections were noted with frontal regions, and negative connections were noted with occipital and parietal regions. The patterns were fairly consistent across the four hemispheric configurations (i.e., LL, LR, RL, and RR).

Hierarchical classification

Hierarchical groupings by hemispheric configuration (i.e., LL, LR, RL, and RR) also revealed differential patterns in the frequency of positive and negative connections between regions (Fig. 6). Within a given functional classification (e.g., primary regions with other primary regions), significant connections were mostly positive. In particular, limbic regions (amygdala and hippocampus) were highly connected with each other. Among connections between regions with different functional classifications, connections between primary and unimodal regions and between paralimbic and limbic regions demonstrated the greatest positive connectivity. On the other hand, the majority of negative connections were observed among heteromodal regions, in particular those paired with primary and unimodal regions. Again, these patterns applied to both intra- and interhemispheric configurations.

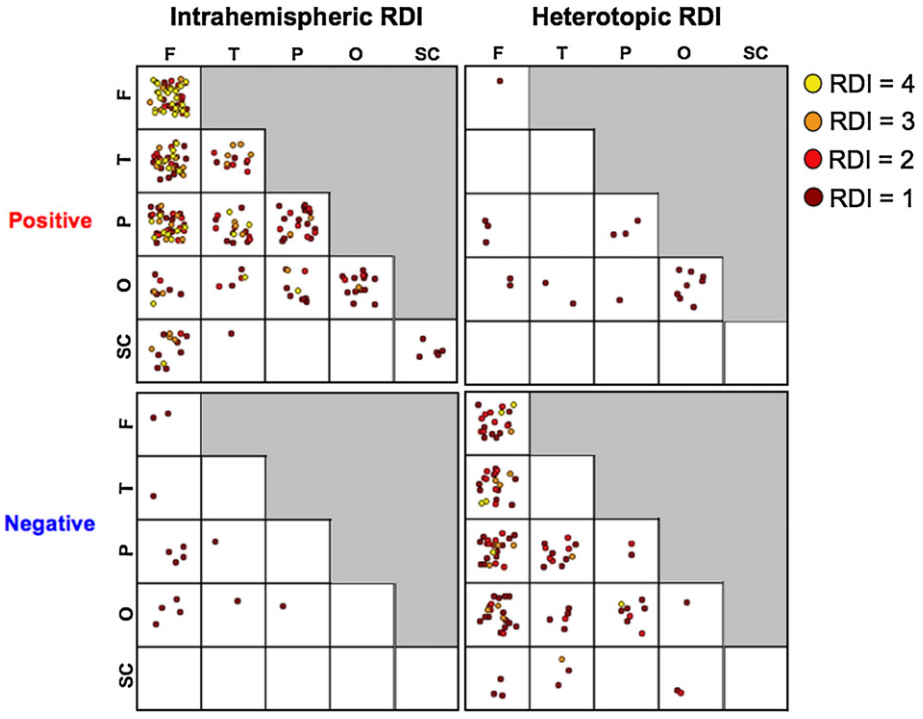

Fig. 4. Localizing intrahemispheric and heterotopic dominance: lobar classification. Regional pairings exhibiting either intrahemispheric dominance (intrahemispheric RDI of 1 or higher) or heterotopic dominance (heterotopic RDI of 1 or higher) were sorted based upon lobe (F = frontal, T = temporal, P = parietal, O = occipital, and SC = subcortical). Positively and negatively connected pairings are illustrated separately, as intrahemispheric dominance was primarily noted for positively connected pairings, and heterotopic dominance was primarily noted for negatively connected pairings. These results indicate that regional pairings were stronger within the hemispheres for positive connections and stronger between the hemispheres for negative connections.

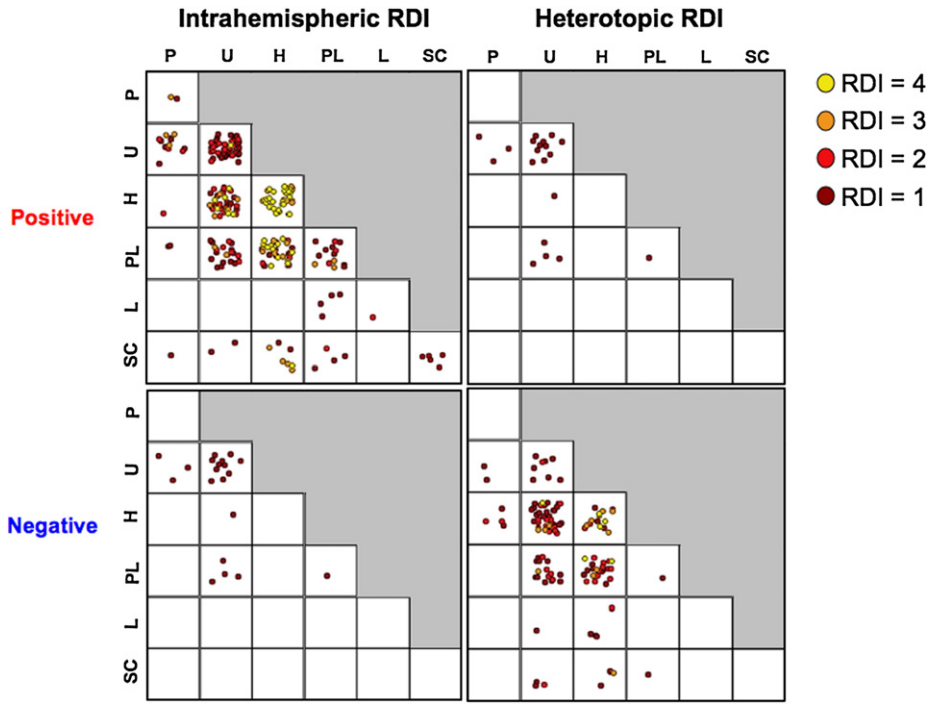

Fig. 5. Localizing intrahemispheric and heterotopic dominance: hierarchical classification. Regional pairings exhibiting either intrahemispheric dominance (intrahemispheric RDI of 1 or higher) or heterotopic dominance (heterotopic RDI of 1 or higher) were sorted based upon functional hierarchy (P = primary sensory-motor areas, U = unimodal association areas, H = heteromodal association areas, PL = paralimbic areas, L = limbic areas, and SC = subcortical). Positively and negatively connected pairings are illustrated separately, as intrahemispheric dominance was primarily noted for positively connected pairings, and heterotopic dominance was primarily noted for negatively connected pairings.

Effect of inter-regional distance

In considering possible confounds associated with the comparison of intrahemispheric and heterotopic connectivity, a notable concern arises from the fact that for a given regional pairing (A and B), the heterotopic configuration will consistently be associated with a greater inter-regional distance than the intrahemispheric configuration, due to hemispheric separation. Prior work has suggested that, at least in part, greater distance between regions is associated with weaker connectivity (Salvador et al., 2005; Honey et al., 2009). This relationship may therefore explain the observed differences in

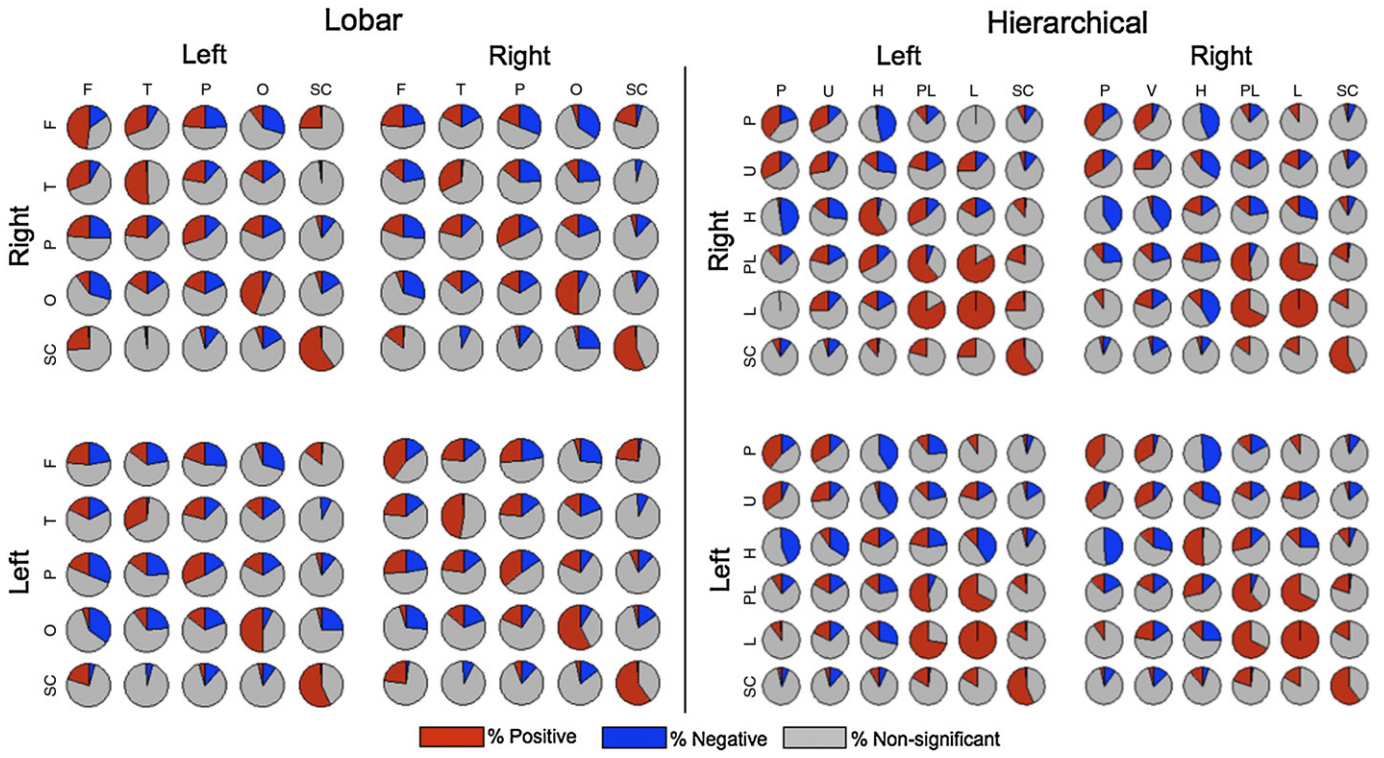

Fig. 6. Distribution of significant connections: lobar and hierarchical classifications. For each of the two regional classification systems (lobar and hierarchical), we depict the regional distribution of the percentage of positive, negative, and non-significant connections (homotopic connections excluded) across the four hemispheric configurations (LL, LR, RL, and RR; 1540 connections per configuration). Highly consistent patterns of connectivity were observed across the four hemispheric configurations, regardless of classification system.

strength of connectivity between the two configurations for positive connections.

In order to address this concern, we first verified the association between inter-regional distance and functional connectivity using intrahemispheric configurations. We found that for positively correlated regional pairs within the same hemisphere, the greater the distance between two regions, the weaker the correlation ($r(LL, dist) = 0.3$, $p < 5 \times 10^{-9}$; $r(RR, dist) = 0.3$, $p < 5 \times 10^{-9}$) — as previously reported by Salvador et al. (2005) and Honey et al. (2009). Next, we addressed the issue of whether or not the additional distance inherent to heterotopic connections (i.e., distance [heterotopic configuration]–distance [intrahemispheric configuration]) can explain differences in connectivity strength observed between intrahemispheric and heterotopic connections. Across regional pairings, no significant relationship was observed between the distance introduced by callosal segregation (distance [heterotopic configuration]–distance [intrahemispheric configuration]) and differences in either positive or negative connectivity strength observed between intrahemispheric and heterotopic connections. We further verified the independent contributions of hemispheric configuration using multiple regression. Specifically, we regressed RSFC for eligible pairings on hemispheric configuration and distance, across positive and negative connections. Distance and hemispheric configuration (intrahemispheric and heterotopic) were both found to be significant predictors of connectivity strength (distance: $beta = -0.0019$, $p < 1.1 \times 10^{-31}$; configuration: $beta = -0.009$, $p < 4.3 \times 10^{-5}$). In sum, our findings suggest that differences in functional connectivity strength between intrahemispheric and heterotopic configurations cannot be explained by distance.

Effect of global signal correction

Some recent studies have suggested that global signal correction may artifactually induce negative correlations in functional connectivity analyses (Murphy et al., 2009; Skudlarski et al., 2008). This raises the possibility that our findings of greater segregation (i.e., negative connectivity) between the hemispheres may be artifactual in origin. In order to address this concern, we re-analyzed our data without global signal correction. As expected, without global signal correction, there were few negative connections. Instead, the majority of connections ranged in strength between 0 and 1. Despite this shift in range, when we examined the regional pairings that exhibited significant negative connectivity when analyzed with global signal correction, we found that heterotopic configurations continued to exhibit greater segregation than intrahemispheric configurations, even without global signal correction. Specifically, we found that for these pairings, connectivity was more weakly positive between the hemispheres than within them (see Supplemental Fig. 7). The absence of global signal correction did not otherwise influence our findings.

Discussion

By using RSFC to provide a comprehensive characterization of patterns of connectivity within (intrahemispheric) and between (heterotopic) the cerebral hemispheres, we noted marked differences with respect to connectivity strength. Specifically, positive intrahemispheric connections tended to be stronger than their corresponding heterotopic connections. In contrast, negative intrahemispheric connections tended to be weaker than their corresponding heterotopic connections. These differential patterns of connectivity were primarily evident among pairings involving frontal and heteromodal regions. As discussed below, we believe that the differences in connectivity strength reflect the hemispheric independence and specialization that form the foundation of leading models of interhemispheric interaction. We also confirmed prior work (Damoiseaux et al., 2006; Di Martino et al., 2008; Margulies et al., 2007) suggesting that the two hemispheres are largely alike in terms of their patterns of RSFC (i.e., the distribution of positive or negative functional connectivity, or lack of significant relationships) and extended this observation to lobar and hierarchical analyses.

Our findings of greater positive connectivity within hemispheres rather than between hemispheres were most salient for connections among heteromodal regions. This may reflect the higher degree of hemispheric specialization commonly associated with higher-order regions (Toga and Thompson, 2003). Consistent with this notion, connections between heteromodal regions and other heteromodal regions and between heteromodal with unimodal and paralimbic regions showed the greatest differences in strength between intrahemispheric and heterotopic configurations. Primary sensory and limbic regions did not evince differential connectivity strengths within or between hemispheres. These findings complement our prior work showing that heteromodal regions have the lowest degree of homotopic connectivity, likely reflecting their tendency to operate more independently than primary regions (Stark et al., 2008). High levels of synchrony might be integral to basic processing of sensory inputs, while decreases in correlation between associative and higher-order regions might reflect greater flexibility required for higher-order processing. For instance, prior work suggests that inter-regional coordination might shift depending on task demands (Hampson et al., 2006). In this way, functional connectivity might reflect functional specialization of brain regions.

We suggest that the greater strength of negative correlations among heterotopic connections, relative to intrahemispheric connections, reflects greater functional segregation between, relative to within hemispheres. Such findings are consistent with work that has hypothesized the hemispheres to be separate processing modules (Friedman and Polson, 1981; Hellige et al., 1979) that either interact via a horse-race model (Bisiacchi et al., 1994) or at times in an inhibitory manner (Chiarello and Maxfield, 1996). Models of interhemispheric interaction emphasize that such segregation is important because it allows the hemispheres to be "shielded" from one another to prevent potential interference during competing tasks or processing (Hoptman and Davidson, 1994; Kosslyn et al., 1992; Liederman and Meehan, 1986). Further, experimental findings using dual-task paradigms demonstrate the advantage of dividing input between the hemispheres (Liederman, 1986; Merola and Liederman, 1985). In addition, prior work suggests that reduced interhemispheric and increased intrahemispheric connectivity are associated with the evolution of larger brain size in primates (Rilling and Insel, 1999).

Such interhemispheric segregation may improve performance for various reasons. For example, computational analyses and computer simulations suggest that representations that code for both coordinate and categorical spatial relationships are best handled when the processes are divided between the hemispheres, with categorical processing performed by the left hemisphere and coordinate processing performed by the right hemisphere (Kosslyn et al., 1992). Chiarello and Maxfield (1996) considered the need for regulatory mechanisms between the hemispheres to coordinate "unified performance from a bilateral system capable of producing simultaneous, and potentially conflicting, outputs" (p. 82). Indeed, evidence for improved performance when the hemispheres perform independently has been reported in both split-brain patients (Ellenberg and Sperry, 1979; Holtzman and Gazzaniga, 1985) and in healthy volunteers (Banich and Belger, 1990; Dimond and Beaumont, 1971).

One particular theory, the Functional Cerebral Distance Model, posits that interference between disparate tasks is minimized when they depend on functionally distant brain regions (Kinsbourne and Hicks, 1978). Consistent with this notion, our lobar analyses for negative connections found greater negative connectivity strength between frontal regions and posterior regions in temporal, parietal, and occipital cortices. Additionally, our analyses of functional hierarchy suggest that hemispheric separation affords greater segregation of processing for heteromodal, paralimbic, and unimodal regions compared to primary, limbic, and subcortical regions.

Still, it is equally important to note how similar the two hemispheres are with respect to functional architecture. The presence of grossly similar functional architectures in the two hemispheres is not necessarily surprising, given that both hemispheres have been found to be capable of performing most cognitive tasks that have been examined, with the exception of speech output (Sperry, 1974) and phonological processing (i.e., rhyming) (Zaidel and Peters, 1981). Likewise, prominent models of interhemispheric interaction such as parallel processing (Banich, 2003) and the horse-race model (Bisiacchi et al., 1994) emphasize the similar abilities of each hemisphere. However, our results do not exclude subtler forms of hemispheric specialization that may depend on cytoarchitectural specializations or differential connectivities to subcortical regions, and which are not addressed by our RSFC data.

Further delineating the mechanisms underlying interhemispheric integration may have critical clinical implications, since interhemispheric differences or asymmetries have been implicated in a number of neurological and psychiatric disorders, including autism (Coben et al., 2008; Nyden et al., 2004), attention-deficit/hyperactivity disorder (Clarke et al., 2008; Garvey et al., 2005), schizophrenia (Liang et al., 2006; Spencer et al., 2003), amyotrophic lateral sclerosis (Karandreas et al., 2007), multiple sclerosis (Lowe et al., 2008), depression (Bajwa et al., 2008), dyslexia (Wijers et al., 2005), and Alzheimer's Disease (Lakmache et al., 1998; Pogarell et al., 2005). Even in our sample of healthy volunteers, we found substantial inter-individual variability in RSFC patterns. If taken to an extreme, as might be the case with the aforementioned disorders, such disruptions may reflect various types of abnormality, such as poorly segregated interhemispheric RSFC networks. Examining resting-state heterotopic functional connectivity is likely to be informative in characterizing impaired interhemispheric interactions in these and other clinical populations.

Whole-brain analyses of interhemispheric correlations at rest also could be particularly important for future research on brain function in elderly populations. Greater bilateral activation is one of the most common imaging findings in the aging brain (Cabeza, 2002). While these activations have sometimes been considered compensatory (Grady and Craik, 2000), an alternative possibility is that bilaterality reflects compromised interhemispheric coordination. Such "non-selective recruitment" may indicate inappropriate recruitment of processing in the less specialized hemisphere, which can serve as a source of interference (Logan et al., 2002). In this regard, the analyses employed in the current study could effectively be applied to examine potential breakdowns in interhemispheric segregation in the elderly.

One of the current challenges in the resting-state functional connectivity literature is how to best understand the neurophysiological relevance of low frequency fluctuations, and how such fluctuations relate to moment-to-moment brain function. An emerging hypothesis is that the brain's intrinsic functional architecture, formed by low frequency phenomena and their inter-regional correlations, provides a framework for the brain's moment-to-moment responses to the external world (Fox et al., 2005; Raichle, 2010; Smith et al., 2009). Thus, regions that show a high degree of coordination on a moment-to-moment basis may exhibit a similarly high degree of coordinated low frequency fluctuations during rest. In contrast, regions that do not frequently exhibit coordinated activity on a moment-to-moment basis, or which exhibit competitive interactions, may manifest a low degree of coordinated low frequency activity at rest. This conceptualization of RSFC provides one framework through which to view our findings on regional variation and interhemispheric processing. Studies have begun to examine resting-state functional connectivity using electroencephalography (EEG) in humans (Mantini et al., 2007; Monto et al., 2008) and using intracranial neuronal recordings in monkeys (Shmuel and Leopold, 2008; Schölvinck et al., 2010), demonstrating the coalescence of several brain rhythms within large-scale functional networks at rest. In the future, multimodal imaging with fMRI and electrophysiological methods will be crucial for elucidating the neurophysiological basis of low frequency fluctuations at rest.

We examined both positive and negative correlations in spontaneous BOLD signal fluctuations. It is important to acknowledge that the interpretation of negative correlations between brain regions remains a source of debate. Detecting so-called anticorrelations requires global signal correction, a common step in resting-state fMRI analyses (Murphy et al., 2009). However, Murphy et al. suggest that anticorrelations may indicate an initially unrelated temporal relationship (i.e., $r = 0$) that is transformed into a negative relationship by application of global signal correction techniques. Though some authors question global signal correction (Skudlarski et al., 2008), it is also considered a useful way to account for physiological cardiac and respiratory signals (Birn et al., 2006; Fox et al., 2005). Beyond the practical value, recent computational modeling results (Ghosh et al., 2008; Steyn-Ross et al., 2009) and neuronal recordings in the rat brain after dopamine loss (Walters et al., 2007) have demonstrated the emergence of negative correlations between nodes. Of note, recent work suggests that negative correlations reflect a biological rather than an artifactual basis (Fox et al., 2009; Chang and Glover, 2009). Perhaps most exciting is the recent simultaneous recording of intracortical local field potentials during resting-state fMRI scanning in monkeys (Schölvinck et al., 2010), which reported that the global component of the fMRI signal is tightly coupled with underlying neural activity. This implies that the negative connectivity enhanced by global regression may reflect residual relationships, after a universal "yoking" signal has been accounted for. Thus, negative correlations may be more akin to partial correlations. Extension of this work to humans with intracortical electrodes will clarify how to interpret patterns of negative connectivity. Finally, it is worth noting that Shehzad et al. (2009) demonstrated that negative RSFC for key brain regions exhibits moderate to high short-term and long-term test–retest reliability.

While the mechanisms underlying negative correlations remain unknown, we posit that anticorrelations reflect segregation among brain networks. If global signal correction is appropriate, then transcallosal passage increases segregation through greater negative connectivity for a given regional pairing (relative to intrahemispheric connectivity). If global signal correction is omitted, then transcallosal segregation pushes connectivity strength closer to zero. In both cases, segregation is increased between the regional pairings. Hence, we interpret the increased negative correlations between heterotopic regions as consistent with the interhemispheric segregation suggested by numerous models of interhemispheric interaction. This interpretation was supported by a supplemental analysis in which we did not perform global signal correction. Despite an expected shift in the range of correlations observed (from positive and negative to mostly positive), those regional pairings that exhibited significant negative connectivity with global signal correction continued to exhibit ordinal relationships consistent with greater segregation for the heterotopic configuration than intrahemispheric, despite the absence of global signal correction. Specifically, we found that for these pairings, connectivity was more weakly positive between the hemispheres than within the hemispheres (see Supplemental Fig. 7). In other words, the connections exhibiting greater negative connectivity in the presence of global signal correction also showed greater segregation when global signal correction was omitted. Thus, in our analyses with and without global signal correction, segregation between regional pairings was increased for the interhemispheric configuration relative to the intrahemispheric configuration.

Given that functional connectivity between two regions can arise through either monosynaptic or polysynaptic connections (Vincent et al., 2007; Roy et al., 2009; Honey et al., 2009; Margulies et al., 2009), several potential explanations exist for why heterotopic RSFC was more strongly negative than intrahemispheric RSFC. Given that the majority

of long-range cortico-cortical connections in the brain are positive, the presence of direct transcallosal inhibitory connections are an unlikely explanation. One possibility is that negative correlations arise between heterotopic regions via the influence of a third party region. For instance, positive intrahemispheric connections might drive negative homotopic connections, such that region A in the left hemisphere excites region B in the left hemisphere which inhibits region B in the right hemisphere. Another possibility is that interhemispheric segregation arises as a result of subcortical influences. Due to the correlational nature of the analyses employed here, investigating these possibilities and directional inter-regional influences posited by various interhemispheric models is beyond the scope of this paper. However, future work would benefit from examining these competing explanations using alternative approaches, such as effective connectivity (Friston, 1994). Moreover, it is important to exercise caution in interpreting negative connectivity as a reflection of direct inhibitory relationships, in the absence of supporting electrophysiological evidence. In addition, prior work (Honey et al., 2009) suggests that patterns of anticorrelation can emerge in the absence of direct inhibitory connections between regions. Similar to the findings of the present work, global signal regression was required to appreciate the bulk of these negative relationships.

In prior work we have addressed some of the potential limitations related to using anatomic parcellation units (Stark et al., 2008). Specifically, we found that volumetric differences in regional masks and probability-weighting did not significantly alter the strength of observed correlations. Furthermore, we demonstrated that susceptibility artifacts cannot account for regional variations in correlation strength. Of note, the use of parcellation units and regional classification systems necessitates some degree of information loss, as large areas of cortex are combined. For example, prior research has demonstrated both compensatory and highly specialized modes of interhemispheric processing among the left and right parietal lobes (Sack et al., 2005). While more detailed regional analyses were beyond the scope of the present study, future work would benefit from the use of an even more detailed and individual-specific method of parcellation (Cohen et al., 2008) and from more region-specific analyses. Further studies are also needed to understand the mechanisms underlying RSFC. In particular, it remains unknown whether observed RSFC reflects direct cortico-cortical connections (Johnston et al., 2008), or whether RSFC is subcortically mediated as suggested by a recent examination of a split-brain patient (Uddin et al., 2008).

In summary, in-depth analyses of heterotopic interhemispheric connectivity allowed us to characterize the patterns of functional connectivity between heterotopic and intrahemispheric regions. We found striking differences in the strength of positive and negative connections across and within the hemispheres, particularly involving frontal and heteromodal regions. This method may prove useful for analyzing developmental trajectories and potential clinical disruptions of interhemispheric processing.

Acknowledgments

This research was sponsored by grants to F.X.C. from NIMH (R01MH083246), the Stavros S. Niarchos Foundation, the Leon Levy Foundation, NARSAD (The Mental Health Research Association) and gifts from Linda and Richard Schaps, and from Jill and Bob Smith.

Appendix A. Supplementary data

Supplementary data associated with this article can be found, in the online version, at doi:10.1016/j.neuroimage.2010.05.073.

References

Andersson, J.L.R., Jenkinson, M., Smith, S.M. 2007a. Non-linear optimisation. FMRIB technical report TR07JA1.

Andersson, J.L.R., Jenkinson, M., Smith, S.M. 2007b. Non-linear registration, aka spatial normalisation. FMRIB technical report TR07JA2.

Bajwa, S., Bermpohl, F., Rigonatti, S.P., Pascual-Leone, A., Boggio, P.S., Fregni, F., 2008. Impaired interhemispheric interactions in patients with major depression. J. Nerv. Ment. Dis. 196, 671–677.

Banich, M.T., 2003. Interaction between the hemispheres and its implications for the processing capacity of the brain, In: Davidson, R., Hugdahl, K. (Eds.), Brain Asymmetry, 2nd edition. MIT Press, Cambridge, MA, pp. 261–302.

Banich, M.T., Belger, A., 1990. Interhemispheric interaction — how do the hemispheres divide-and-conquer a task. Cortex 26, 77–94.

Banich, M.T., Brown, W.S., 2000. A life-span perspective on interaction between the cerebral hemispheres. Dev. Neuropsychol. 18, 1–10.

Birn, R.M., Diamond, J.B., Smith, M.A., Bandettini, P.A., 2006. Separating respiratory-variation-related neuronal-activity-related fluctuations in fluctuations from fMRI. Neuroimage 31, 1536–1548.

Bisiacchi, P., Marzi, C.A., Nicoletti, R., Carena, G., Mucignat, C., Tomaiuolo, F., 1994. Left–right asymmetry of callosal transfer in normal human-subjects. Behav. Brain Res. 64, 173–178.

Biswal, B., Yetkin, F.Z., Haughton, V.M., Hyde, J.S., 1995. Functional connectivity in the motor cortex of resting human brain using echo-planar MRI. Magn. Reson. Med. 34, 537–541.

Cabeza, R., 2002. Hemispheric asymmetry reduction in older adults: the HAROLD model. Psychol. Aging 17, 85–100.

Chang, C., Glover, G.H., 2009. Effects of model-based physiological noise correction on default mode network anti-correlations and correlations. Neuroimage 47 (4), 1448–1459.

Chiarello, C., Maxfield, L., 1996. Varieties of interhemispheric inhibition, or how to keep a good hemisphere down. Brain Cogn. 30, 81–108.

Clarke, A.R., Barry, R.J., Heaven, P.C.L., McCarthy, R., Selikowitz, M., Byrne, M.K., 2008. EEG coherence in adults with attention-deficit/hyperactivity disorder. Int. J. Psychophysiol. 67, 35–40.

Coben, R., Clarke, A.R., Hudspeth, W., Barry, R.J., 2008. EEG power and coherence in autistic spectrum disorder. Clin. Neurophysiol. 119, 1002–1009.

Cohen, A.L., Fair, D.A., Dosenbach, N.U.F., Miezin, F.M., Dierker, D., Van Essen, D.C., Schlaggar, B.L., Petersen, S.E., 2008. Defining functional areas in individual human brains using resting functional connectivity MRI. Neuroimage 41, 45–57.

Damoiseaux, J.S., Rombouts, S.A.R.B., Barkhof, F., Scheltens, P., Stam, C.J., Smith, S.M., Beckmann, C.F., 2006. Consistent resting-state networks across healthy subjects. Proc. Natl. Acad. Sci. USA 103, 13848–13853.

Di Martino, A., Scheres, A., Margulies, D.S., Kelly, A.M.C., Uddin, L.Q., Shehzad, Z., Biswal, B., Walters, J.R., Castellanos, F.X., Milham, M.P., 2008. Functional connectivity of human striatum: a resting state fMRI study. Cereb. Cortex 18, 2735–2747.

Dimond, S., Beaumont, G., 1971. Use of 2 cerebral hemispheres to increase brain capacity. Nature 232 270-&.

Ellenberg, L., Sperry, R.W., 1979. Capacity for holding sustained attention following commissurotomy. Cortex 15, 421–438.

Fair, D.A., Cohen, A.L., Dosenbach, N.U.F., Church, J.A., Miezin, F.M., Barch, D.M., Raichle, M.E., Petersen, S.E., Schlaggar, B.L., 2008. The maturing architecture of the brain's default network. Proc. Natl. Acad. Sci. USA 105, 4028–4032.

Fair, D.A., Dosenbach, N.U.F., Church, J.A., Cohen, A.L., Brahmbhatt, S., Miezin, F.M., Barch, D.M., Raichle, M.E., Petersen, S.E., Schlaggar, B.L., 2007. Development of distinct control networks through segregation and integration. Proc. Natl. Acad. Sci. USA 104, 13507–13512.

Fox, M.D., Snyder, A.Z., Vincent, J.L., Corbetta, M., Van Essen, D.C., Raichle, M.E., 2005. The human brain is intrinsically organized into dynamic, anticorrelated functional networks. Proc. Natl. Acad. Sci. USA 102, 9673–9678.

Fox, M.D., Zhang, D., Snyder, A.Z., Raichle, M.E., 2009. The global signal and observed anticorrelated resting state brain networks. J. Neurophysiol. 101, 3270–3283.

Friedman, A., Polson, M.C., 1981. Hemispheres as independent resource systems — limited-capacity processing and cerebral specialization. J. Exp. Psychol. Hum. Percept. Perform. 7, 1031–1058.

Friston, K.J., 1994. Functional and effective connectivity in neuroimaging: a synthesis. Hum. Brain Mapp. 2, 56–78.

Garvey, M.A., Barker, C.A., Bartko, J.J., Denckla, M.B., Wassermann, E.M., Castellanos, F.X., Dell, M.L., Ziemann, U., 2005. The ipsilateral silent period in boys with attention-deficit/hyperactivity disorder. Clin. Neurophysiol. 116, 1889–1896.

Ghosh, A., Rho, Y., McIntosh, A.R., Kotter, R., Jirsa, V.K., 2008. Noise during rest enables the exploration of the brain's dynamic repertoire. PLoS Comput. Biol. 4.

Grady, C.L., Craik, F.I., 2000. Changes in memory processing with age. Curr. Opin. Neurobiol. 10, 224–231.

Hampson, M., Driesen, N.R., Skudlarski, P., Gore, J.C., Constable, R.T., 2006. Brain connectivity related to working memory performance. J. Neurosci. 26, 13338–13343.

Hagmann, P., Cammoun, L., Gigandet, X., Meuli, R., Honey, C.J., Wedeen, V., Sporns, O., 2008. Mapping the structural core of human cerebral cortex. PLoS Biol. 6, 1479–1493.

Hellige, J.B., Cox, P.J., Litvac, L., 1979. Information-processing in the cerebral hemispheres — selective hemispheric activation and capacity limitations. J. Exp. Psychol. Gen. 108, 251–279.

Holtzman, J.D., Gazzaniga, M.S., 1985. Enhanced dual task-performance following corpus commissurotomy in humans. Neuropsychologia 23, 315–321.

Honey, C.J., Sporns, O., Cammoun, L., Gigandet, X., Thiran, J.P., Meuli, R., Hagmann, P., 2009. Predicting human resting-state functional connectivity from structural connectivity. Proc. Natl. Acad. Sci. USA 106, 2035–2040.

Hoptman, M.J., Davidson, R.J., 1994. How and why do the 2 cerebral hemispheres interact. Psychol. Bull. 116, 195–219.

Jenkinson, M., Smith, S., 2001. A global optimisation method for robust affine registration of brain images. Med. Image Anal. 5, 143–156.

Jenkinson, M., Bannister, P., Brady, M., Smith, S., 2002. Improved optimization for the robust and accurate linear registration and motion correction of brain images. Neuroimage 17, 825–841.
Johnston, J.M., Vaishnavi, S.N., Smyth, M.D., Zhang, D.Y., He, B.J., Zempel, J.M., Shimony, J.S., Snyder, A.Z., Raichle, M.E., 2008. Loss of resting interhemispheric functional connectivity after complete section of the corpus callosum. J. Neurosci. 28, 6453–6458.
Karandreas, N., Papadopoulou, M., Kokotis, P., Papapostolou, A., Tsivgoulis, G., Zambelis, T., 2007. Impaired interhemispheric inhibition in amyotrophic lateral sclerosis. Amyotroph. Lateral Scler. 8, 112–118.
Kelly, A.M.C., Uddin, L.Q., Biswal, B.B., Castellanos, F.X., Milham, M.P., 2008. Competition between functional brain networks mediates behavioral variability. Neuroimage 39, 527–537.
Kelly, A.M.C., de Zubicaray, G., Di Martino, A., Copland, D.A., Reiss, P.T., Klein, D.F., Castellanos, F.X., Milham, M.P., McMahon, K., 2009. L-dopa modulates functional connectivity in striatal cognitive and motor networks: a double-blind placebo-controlled study. J. Neurosci. 29 (22), 7364–7378.
Kennedy, D.N., Lange, N., Makris, N., Bates, J., Meyer, J., Caviness, V.S., 1998. Gyri of the human neocortex: an MRI-based analysis of volume and variance. Cereb. Cortex 8, 372–384.
Kinsbourne, M., Hicks, R.E., 1978. Mapping cerebral functional space: competition and collaboration in human performance. In: Kinsbourne, M. (Ed.), Asymmetrical Function of the Brain. Cambridge University Press, Cambridge, pp. 267–273.
Kosslyn, S.M., Chabris, C.F., Marsolek, C.J., Koenig, O., 1992. Categorical versus coordinate spatial relations — computational analyses and computer-simulations. J. Exp. Psychol. Hum. Percept. Perform. 18, 562–577.
Lakmache, Y., Lassonde, M., Gauthier, S., Frigon, J.Y., Lepore, F., 1998. Interhemispheric disconnection syndrome in Alzheimer's disease. Proc. Natl. Acad. Sci. USA 95, 9042–9046.
Liang, M., Zhou, Y., Jiang, T.Z., Liu, Z.N., Tian, L.X., Liu, H.H., Hao, Y.H., 2006. Widespread functional disconnectivity in schizophrenia with resting-state functional magnetic resonance imaging. NeuroReport 17, 209–213.
Liederman, J., 1986. Subtraction in addition to addition — dual task-performance improves when tasks are presented to separate hemispheres. J. Clin. Exp. Neuropsychol. 8, 486–502.
Liederman, J., Meehan, P., 1986. When is between-hemisphere division-of-labor advantageous. Neuropsychologia 24, 863–874.
Liu, H., Stufflebeam, S.M., Sepulcre, J., Hedden, T., Buckner, R.L., 2009. Evidence from intrinsic activity that asymmetry of the human brain is controlled by multiple factors. Proc. Natl. Acad. Sci. USA 106, 20499–20503.
Logan, J.M., Sanders, A.L., Snyder, A.Z., Morris, J.C., Buckner, R.L., 2002. Under-recruitment and nonselective recruitment: dissociable neural mechanisms associated with aging. Neuron 33, 827–840.
Lowe, M.J., Beall, E.B., Sakaie, K.E., Koenig, K.A., Stone, L., Marrie, R.A., Phillips, M.D., 2008. Resting state sensorimotor functional connectivity in multiple sclerosis inversely correlates with transcallosal motor pathway transverse diffusivity. Hum. Brain Mapp. 29, 818–827.
Makris, N., Meyer, J.W., Bates, J.F., Yeterian, E.H., Kennedy, D.N., Caviness, V.S., 1999. MRI-based topographic parcellation of human cerebral white matter and nuclei II. Rationale and applications with systematics of cerebral connectivity. NeuroImage 9, 18–45.
Mantini, D., Perrucci, M.G., Del Gratta, C., Romani, G.L., Corbetta, M., 2007. Electrophysiological signatures of resting state networks in the human brain. Proc. Natl. Acad. Sci. USA 104 (32), 13170–13175.
Margulies, D.S., Kelly, A.M.C., Uddin, L.Q., Biswal, B.B., Castellanos, F.X., Milham, M.P., 2007. Mapping the functional connectivity of anterior cingulate cortex. Neuroimage 37, 579–588.
Margulies, D.S., Vincent, J.L., Kelly, C., Lohmann, G., Uddin, L.Q., Biswal, B.B., Villringer, A., Castellanos, F.X., Milham, M.P., Petrides, M., 2009. Precuneus shares intrinsic functional architecture in humans and monkeys. Proc. Natl. Acad. Sci. USA 106, 20069–20074.
Merola, J.L., Liederman, J., 1985. Developmental-changes in hemispheric independence. Child Dev. 56, 1184–1194.
Mesulam, M.M., 2000. Principles of Behavioral and Cognitive Neurology. Oxford University Press, New York.
Monto, S., Palva, S., Voipio, J., Palva, J.M., 2008. Very slow EEG fluctuations predict the dynamics of stimulus detection and oscillation amplitudes in humans. J. Neurosci. 28 (33), 8268–8272.
Murphy, K., Birn, R.M., Handwerker, D.A., Jones, T.B., Bandettini, P.A., 2009. The impact of global signal regression on resting state correlations: are anti-correlated networks introduced? Neuroimage 44, 893–905.
Nyden, A., Carlsson, M., Carlsson, A., Gillberg, C., 2004. Interhemispheric transfer in high-functioning children and adolescents with autism spectrum disorders: a controlled pilot study. Dev. Med. Child Neurol. 46, 448–454.
Pogarell, O., Teipel, S.J., Juckel, G., Gootjes, L., Moller, T., Burger, K., Leinsinger, G., Moller, H.J., Hegerl, U., Hampel, H., 2005. EEG coherence reflects regional corpus callosum area in Alzheimer's disease. J. Neurol. Neurosurg. Psychiatry 76, 109–111.
Raichle, M.E., 2010. Two views of brain function. Trends Cogn. Sci. 14 (4), 180–190.
Rilling, J.K., Insel, T.R., 1999. Differential expansion of neural projection systems in primate brain evolution. NeuroReport 10, 1453–1459.
Roy, A.K., Shehzad, Z., Margulies, D.S., Kelly, A.M., Uddin, L.Q., Gotimer, K., Biswal, B.B., Castellanos, F.X., Milham, M.P., 2009. Functional connectivity of the human amygdala using resting state fMRI. Neuroimage 45, 614–626.
Sack, A.T., Camprodon, J.A., Pascual-Leone, A., Goebel, R., 2005. The dynamics of interhemispheric compensatory processes in mental imagery. Science 308, 702–704.
Salvador, R., Suckling, J., Coleman, M.R., Pickard, J.D., Menon, D., Bullmore, E., 2005. Neurophysiological architecture of functional magnetic resonance images of human brain. Cereb. Cortex 15, 1332–1342.
Schölvinck, M.L., Maier, A., Ye, F.Q., Duyn, J.H., Leopold, D.A., 2010. Neural basis of global resting-state fMRI activity. Proc. Natl. Acad. Sci. USA 107 (22), 10238–10243.
Shehzad, Z., Kelly, A.M.C., Reiss, P.T., Gee, D.G., Gotimer, K., Uddin, L.Q., Lee, S.H., Margulies, D.S., Roy, A.K., Biswal, B.B., Petkova, E., Castellanos, F.X., Milham, M.P., 2009. The resting brain: unconstrained yet reliable. Cereb. Cortex 19 (10), 2209–2229.
Shmuel, A., Leopold, D.A., 2008. Neuronal correlates of spontaneous fluctuations in fMRI signals in monkey visual cortex: implications for functional connectivity at rest. Hum. Brain Mapp. 29 (7), 751–761.
Skudlarski, P., Jagannathan, K., Calhoun, V.D., Hampson, M., Skudlarska, B.A., Pearlson, G., 2008. Measuring brain connectivity: diffusion tensor imaging validates resting state temporal correlations. Neuroimage 43, 554–561.
Smith, S.M., Fox, P.T., Miller, K.L., Glahn, D.C., Fox, P.M., Mackay, C.E., Filippini, N., Watkins, K.E., Toro, R., Laird, A.R., Beckmann, C.F., 2009. Correspondence of the brain's functional architecture during activation and rest. Proc. Natl. Acad. Sci. USA 106 (31), 13040–13045.
Spencer, K.M., Nestor, P.G., Niznikiewicz, M.A., Salisbury, D.F., Shenton, M.E., McCarley, R.W., 2003. Abnormal neural synchrony in schizophrenia. J. Neurosci. 23, 7407–7411.
Sperry, R.W., 1974. Lateral specialization in the surgically separated hemispheres. In: Schmitt, F., Worden, F. (Eds.), The Neurosciences: Third Study Program. MIT Press, Cambridge, MA, pp. 5–19.
Stark, D.E., Margulies, D.S., Shehzad, Z.E., Reiss, P., Kelly, A.M.C., Uddin, L.Q., Gee, D.G., Roy, A.K., Banich, M.T., Castellanos, F.X., Milham, M.P., 2008. Regional variation in interhemispheric coordination of intrinsic hemodynamic fluctuations. J. Neurosci. 28, 13754–13764.
Steyn-Ross, M.L., Steyn-Ross, D.A., Wilson, M.T., Sleigh, J.W., 2009. Modeling brain activation patterns for the default and cognitive states. Neuroimage 45, 298–311.
Toga, A.W., Thompson, P.M., 2003. Mapping brain asymmetry. Nat. Rev. Neurosci. 4, 37–48.
Uddin, L.Q., Mooshagian, E., Zaidel, E., Scheres, A., Margulies, D.S., Kelly, A.M.C., Shehzad, Z., Adelstein, J.S., Castellanos, F.X., Biswal, B.B., Milham, M.P., 2008. Residual functional connectivity in the split-brain revealed with resting-state functional MRI. NeuroReport 19, 703–709.
Vincent, J.L., Patel, G.H., Fox, M.D., Snyder, A.Z., Baker, J.T., Van Essen, D.C., Zempel, J.M., Snyder, L.H., Corbetta, M., Raichle, M.E., 2007. Intrinsic functional architecture in the anaesthetized monkey brain. Nature 447, 83–86.
Walters, J.R., Hu, D., Itoga, C.A., Parr-Brownlie, L.C., Bergstrom, D.A., 2007. Phase relationships support a role for coordinated activity in the indirect pathway in organizing slow oscillations in basal ganglia output after loss of dopamine. Neuroscience 144, 762–776.
Wijers, A.A., Been, P.H., Romkes, K.S., 2005. Dyslexics show a deviant lateralization of attentional control: a brain potential study. Neurosci. Lett. 374, 87–91.
Zaidel, E., Peters, A.M., 1981. Phonological encoding and ideographic reading by the disconnected right-hemisphere — 2 case studies. Brain Lang. 14, 205–234.